Interior Search Optimization Algorithm for Modeling Power Curve of Wind Turbine

Ahmed M. Agwa*, **‡

* Electrical Engineering Department, Faculty of Engineering, Northern Border University, Arar 1321, Saudi Arabia

** Electrical Engineering Department, Faculty of Engineering, Al-Azhar University, Cairo 11651, Egypt

(ah1582009@yahoo.com)

‡ Corresponding Author; Ahmed M. Agwa, Assistant Professor, Electrical Engineering Department, Faculty of Engineering, Northern Border University, Arar 1321, Saudi Arabia, ahmad.agua@nbu.edu.sa

Abstract- Incorrect sensor reading, weather conditions, operation stoppage, and defect, produce noise in the records of wind speed and the synchronized wind turbine (WT) power. This noise still remains even after purification so fitted curve of wind turbine power model (WTPM) may differ from that in the datasheet. WTPM is vital due to its role in managing and predicting wind energy. Identification of WTPM parameters can be addressed as a nonlinear optimization issue. The objective function targets minimizing the root of the mean squared errors (RMSE) among the accompanying computed and measured wind power points with subjection to group of parameters constraints. In this article, a newly designed interior search optimization algorithm (ISA) is applied to identify the WTPM obscure parameters. Three parametric models namely 5- , 6-parameters logistic functions, and amended hyperbolic tangent are analyzed neatly. Simulations are accomplished using MATLAB. The ISA applicability is evaluated via comparing its results with the observed results of two WTs. To legalize the ISA results, they are compared with other methods results. It can be declared here that the ISA performs well and possesses a fine strength to generate WTPM parameters with RMSE less than other approaches by 18.11% to 65.93%.

Keywords Parametric model; power curve; wind turbine; optimization approaches; interior search algorithm.

1. Introduction

In the last decades, exploitation of renewable energy sources (RESs) increases speedily in off-grid and on-grid applications due to their environmental friendliness, sustainability, and economic. Wind energy is a significant RES that is extensive in most sites over the world [1]. The blades of wind turbine (WT) rotate while the wind hits them and they transmit the rotational motion to the generator through gear box [2].

WT datasheets commonly declare speed-power relationship as limited number of scheduled points. These abovementioned points are measured at ordinary atmospheric condition, which is often not the case where a WT is erected, and therefore not enough for administering and predicting wind energy so wind turbine power model (WTPM) needs to be identified [3].

WTPM requires synchronized measuring wind speed and power of WT for a satisfactorily long period to generate a considerable database at different atmospheric conditions. Afterward, knowing such a series of measurements of both the wind speed and the WT power, WTPM estimation, which is scrutinized in this research, becomes accurate.

The techniques utilized to describe WTPM are classified into two categories: parametric that includes equation with parameters and non-parametric that is trained using measured points [4]. The parametric WTPM is preferred due to its low computation cost. Accordingly, the current article addresses parametric WTPM.

The techniques included in the parametric WTPM are least squares [5-7], genetic algorithm [8], evolutionary computation approach [9], differential evolution, particle swarm algorithm [10], highest likelihood estimator [11], cultural algorithm [12], dynamic power curve [13,14], Jaya optimizer [15], Non-linear retraction [16], Monte Carlo approach [17], multi-verse optimizer [18], trajectory sensitivity [19], and boundary element momentum method [20].

The techniques of the non-parametric WTPM are neural networks [21-25], neuro-fuzzy structure [26], fuzzy cluster [27], support vector machine [28,29], Gaussian procedure [30], monotonic retrogression [31].

In connection with the survey mentioned above, and based on the theory of no-free-launch, there exist still an opportunity to ameliorate the extraction of WTPM parameters. For this purpose, this research aims at treatment of the interior search optimization algorithm (ISA), which was created lately, to extract obscure parameters of WTPM. The decoration and interior design, inspired Gandomi to design ISA as a novel meta-heuristic algorithm [32]. Afterwards, ISA has been successfully applied for engineering optimization issues such as operation of big reservoirs systems [33], digital differentiator design [34], optimal power flow [35], and load dispatch [36,37]. Application of ISA has been very successful for detection of fuel cell model parameters [38,39] and photovoltaic model parameters [40]. Therefore, ISA is selected in this current research since its reported results are propitious and confirm its vantage over other optimizers.

This research includes analysis of three parametric models namely five parameters logistic function (5-PLog), six parameters logistic function (6-PLog), and amended hyperbolic tangent (AHTan) which has nine parameters since they don't produce errors about the rated speed like linear, quadratic, and cubic models.

This research owns the following contributions:

➢ Novel application of ISA to optimally identify the obscure parameters of WTPM.

➢ Two WTs are analyzed using three parametric models.

➢ Comparison of ISA with other optimizers based on the results of modeling two WTs.

The paper is ordered as follows: Section 2 illustrates parametric models of WTPM. Section 3 includes formulation of the objective function (F_{ob}) as well as the constraints. ISA is clarified in Section 4. Section 5 discusses the yielded results. Conclusions are abridged in Section 6.

2. Parametric WTPM

Fig. 1 reveals power curve of WT which is characterized by three wind speeds. In detail, they are cut-in speed (v_{cut-in}) at which the power begins to be generated, rated speed (v_n) at which the rated power (P_n) is generated, and cut-off speed $(v_{cut-off})$ at which the brake is operated to avoid the rotor damage [41,42]. In this research, WTPM is modeled using three parametric models: 5-PLog, 6-PLog, and AHTan. On the other hand, linear, quadratic, and cubic models are not utilized since they produce errors about the rated speed [43].
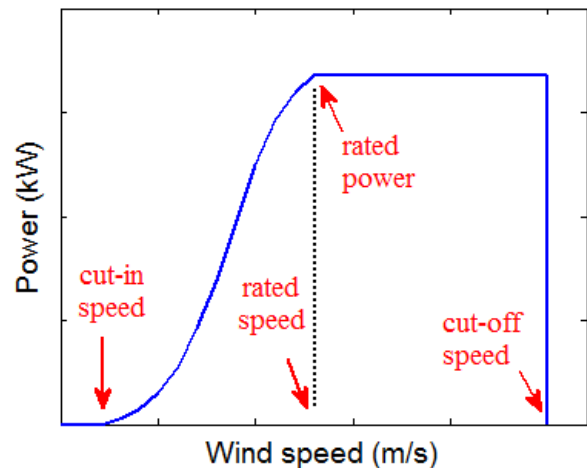

Fig. 1. Power curve of WT

2.1. 5-PLog

Logistic formula with five parameters is utilized to approximate the wind power curve shape as stated in Eq. (1).

$$P(v) = a + \frac{b - a}{\left[1 + \left(\frac{v}{c}\right)^d\right]^g} \tag{1}$$

where $P(v)$ symbolizes the output electrical power at wind speed v and (a, b, c, d, g) are five obscure parameters to be extracted and their meanings are the greatest asymptote, the smallest asymptote, the flexion point, the slope at the flexion point, and the asymmetric coefficient, correspondingly [44].

2.2. 6-PLog

Approximation of the power curve shape using logistic formula with six parameters is indicated in Eq. (2).

$$P(v) = \alpha + \frac{\beta - \alpha}{\left[\lambda + e^{-\gamma(v-\delta)}\right]^{\frac{1}{\xi}}} \tag{2}$$

where $(\alpha, \beta, \gamma, \delta, \xi, \lambda)$ are six unknown parameters to be identified and their meanings are the lower asymptote, the higher asymptote, the rate of growth, a value related to $P(0)$, the nearest asymptote to the greatest growth portion of the curve, and a number randomized around 1, consecutively [29].

2.3. AHTan

The power curve shape is approximated by amended hyperbolic tangent formula with nine parameters as described in Eq. (3).

$$P(v) = h + \frac{m \cdot e^{n \cdot v} - o \cdot e^{p \cdot v}}{q \cdot e^{r \cdot v} - w \cdot e^{z \cdot v}} \tag{3}$$

where $(h, m, n, o, p, q, r, w, z)$ are obscure unknown parameters to be determined and they don't have particular meaning [45].

3. Formularization of the F_{ob} and the constraints

The F_{ob} targets minimizing the root of the mean squared errors (RMSE) among the accompanying computed and measured wind power points for WTPM, as stated in Eq. (4).

$$F_{ob} = min(RMSE)$$
$$= min\left\{\sqrt{\frac{1}{M} \cdot \sum_{k=1}^{M}[P_m(k) - P_c(k)]^2}\right\} \qquad (4)$$

where M symbolizes the measurement points quantity, P_m and P_c symbolize the measured and computed wind power, consecutively.

The constraints which are identified by the bottom and top limits of WTPM parameters, subjugate the F_{ob}.

4. ISA

The idea of ISA is taken from architectonics and mirror work (MiWo) which was orderly method utilized by the Persians to design the decor. To accomplish the aims of decor project, the requests and the income of customer have to be taken into account [33]. The beginning is to design constituents' combination from boundaries toward inside by putting constituents from the walls and shrinking the inside space. During this procedure, constituents' combination is changed to form more beautiful vision and environment (better F_{ob}) conditional on customer satisfaction (constraints). MiWo is wonderful creation in fine arts for decorative design. Different mirrors are utilized in MiWo to create more attractive environment. It is important in this procedure to put the mirrors at the prettiest constituents to emphasize their beautiful. This repeated procedure can be utilized in optimization issues by putting some mirrors at the universal finest (fittest) constituent to get some other pretty views [32]. The constituents other than the fittest are separated into two sets. The first set, named the combination set, is utilized for combination optimization. The second set, named the mirror set, is utilized for mirror search. The key steps for defining the beautiful vision and environment using ISA are as follows:

4.1. 1st Step

The constituents, whose quantity equals population (N_{pop}), are randomly generated between bottom (BB) and top bounds (TB) and their F_{ob} is computed.

4.2. 2nd Step

The universal finest constituent is gotten in iteration i and it is symbolized by x_{uf}^i.

4.3. 3rd Step

The constituents other than x_{uf}^i are separated randomly into two sets (combination set and mirror set), utilizing a threshold value (τ) and a random number (r_1) among 0 and 1 for each constituent. If $r_1 \leq \tau$ then constituent is put in the mirror set; else, it is put in the combination set. Hypothetically, τ is also a number among 0 and 1. Anywise, to balance diversification and intensification, τ has to be adjusted cautiously since it is the only parameter in ISA.

4.4. 4th Step

It is necessary to change slightly the location of the universal finest constituent utilizing the random walk for local search around the universal finest, as formulated in Eq. (5).

$$x_{uf}^i = x_{uf}^{i-1} + m \cdot \sigma \qquad (5)$$

$$\sigma = 0.01(TB - BB) \qquad (6)$$

where m symbolizes a vector includes normally diffused random values and σ symbolizes scale factor.

4.5. 5th Step

Each constituent in the combination set, is randomly changed within its bounds, as stated in Eq. (7).

$$x_j^i = BB_j + r_2 \cdot (TB_j - BB_j) \qquad (7)$$

where r_2 symbolizes random number among 0 and 1 and (x_j^i, TB_j, BB_j) symbolize the constituent j in the iteration i and its bounds, consecutively.

4.6. 6th Step

A mirror is randomly put among each constituent in the mirror set and the universal finest constituent. The mirror location $(x_{m,j}^i)$ for the constituent j in the iteration i, is computed using Eq. (8).

$$x_{m,j}^i = r_3 \cdot x_j^{i-1} + (1 - r_3) \cdot x_{uf}^i \qquad (8)$$

where r_3 symbolizes a random number among 0 and 1. The image position or constituent virtual position relies on the mirror location, as formulated in Eq. (9).

$$x_j^i = 2x_{m,j}^i - x_j^{i-1} \qquad (9)$$

4.7. 7th Step

The F_{ob} of new constituents positions and virtual constituents are computed and positions are updated based on F_{ob} improvement, as formulated in Eq. (10) in case of minimization.

$$x_j^i = \begin{cases} x_j^i & \text{if } F_{ob}^i < F_{ob}^{i-1} \\ x_j^{i-1} & \text{otherwise} \end{cases} \qquad (10)$$

4.8. 8th Step

ISA will be ended if the maximum number of iterations (N_{max}) is reached. Figure 2 demonstrates the flowchart of ISA [35].

Adjusting τ

Adjusting parameters represents an obstacle in all optimizers which usually include two or more parameters. Nevertheless, the ISA distinguishes from other optimizers that it has only one parameter τ, this gives ISA more adaptation to a wider group of optimization issues. For unconstrained optimization issues, τ has a fixed value of

0.25. For exploration at the beginning of constrained optimization issues, combination leads mirror search. For exploitation when the iteration number (i) approaches N_{max}, mirror search gradually leads combination. Thus the value of τ is required to increase as i increases towards N_{max} [46]. In this paper, τ value is determined using Eq. (11) during optimization iterations. This means that τ is adjusted automatically which adds second advantage to ISA.
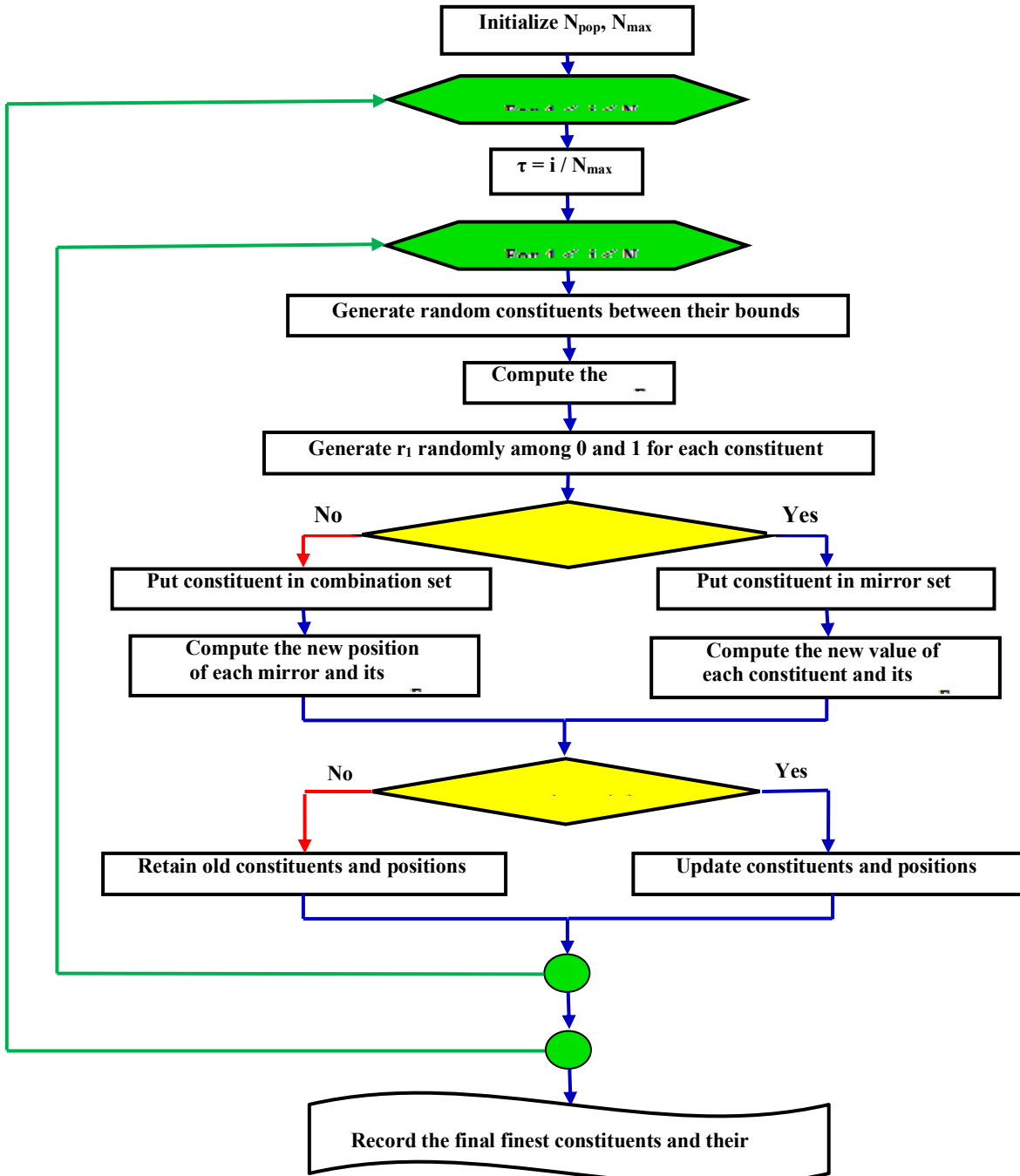
$$\tau = \frac{i}{N_{max}} \tag{11}$$

Fig. 2. Flowchart of ISA

5. Results and discussions

Two cases are studied for assessment of the efficacy of the suggested ISA-based approach in identifying WTPM

parameters. The studied WTs are Bazán 62/1300 and Nordex N117/3600, whose data were measured in Spain throughout 2019 and Turkey throughout 2018, respectively. 5-PLog, 6-PLog, and AHTan models are employed in this article. The specifications of two WTs are summarized in Table 1.

Table 1. Specifications of WTs

Model	Bazán 62/1300	Nordex N117/3600
P_n (MW)	1.3	3.6
v_{cut-in} (m/s)	3	3
v_n (m/s)	15	13
$v_{cut-off}$ (m/s)	25	25
Rotor diameter (m)	62	116.8
Hub height (m)	50	76
Voltage (V)	690	660
Frequency (Hz)	50	50

The maximum iterations are 150 and the population quantity is 20. Since the ISA is one from heuristic-based optimizers which are described as high stochastic, it is required to run ISA numerous independent times for getting minimum F_{ob} and corresponding WTPM parameters.

Extracted WTPM parameters using 5-PLog, 6-PLog, and AHTan are revealed in Tables 2, 3 and 4, consecutively. The diagrams of RMSE convergence are revealed in Figs. 3 and 4.

Table 2. Extracted WTPM parameters using 5-PLog

Model / Parameter	Bazán 62/1300	Nordex N117/3600
a	−2.9806	−2.0809
b	224.8731	373.5613
c	12.3084	11.0472
d	−5.4556	−10
g	0.4395	0.2961

Literature doesn't contain results about Bazán 62/1300 and Nordex N117/3600 which are studied in this article. To legalize the ISA results, two other optimizers are utilized namely atom search optimizer (ASO) and mining blast optimizer (MBO) with $N_{max} = 150$ and $N_{pop} = 20$ as adjusted in ISA for fair comparison. Comparisons among ISA, ASO, and MBO in accordance with their results, manifest that the yielded RMSE by ISA is smaller than that of other optimizers by 18.11% to 65.93%, as displayed in Figs. 3, 4, Tables 5, and 6. To visually compare among the results of three parametric models namely 5-PLog, 6-PLog, and AHTan which are gotten using ISA, their RMSE convergences are plotted in the same diagram as displayed in Fig. 5. It can be noticed from Tables 5, 6, and Fig. 5, that the

6-PLog model has the smallest RMSE and the fastest convergence.

Table 3. Extracted WTPM parameters using 6-PLog

Model / Parameter	Bazán 62/1300	Nordex N117/3600
α	−26.5463	-28.9961
β	149.9157	374.4131
γ	0.5000	0.9963
δ	10.0938	10.7488
ξ	2.1549	3.1836
λ	0.5000	1.0735

Table 4. Extracted WTPM parameters using AHTan

Model / Parameter	Bazán 62/1300	Nordex N117/3600
h	−0.2943	−0.4626
m	0.3849	0.6734
n	−0.1666	0.2214
o	0.6807	−0.1046
p	−0.5375	−0.1696
q	−0.3394	0.1867
r	0.0149	−0.2833
w	0.0049	−0.0017
z	−0.5120	−0.2261

Table 5. RMSE of Bazán 62/1300 compared to other optimizers

Algorithm	ASO	MBO	ISA
5-PLog	0.177636	0.153891	0.112980
6-PLog	0.132573	0.127577	0.108789
AHTan	0.199612	0.183254	0.113243

Table 6. RMSE of Bazán 62/1300 compared to other optimizers

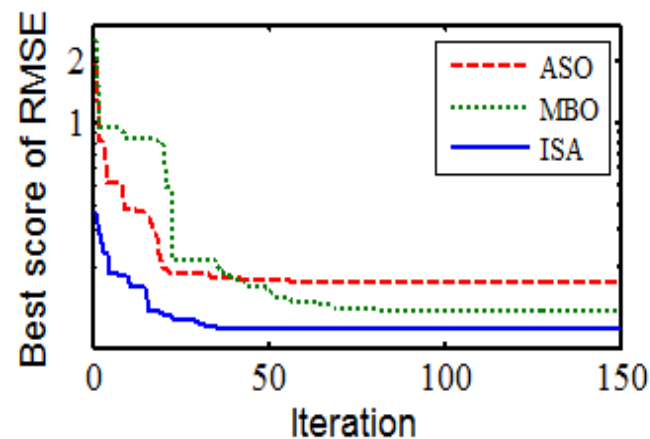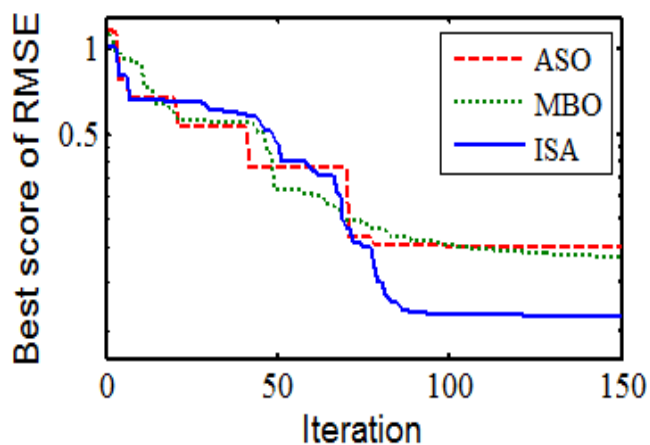| Algorithm	ASO	MBO	ISA
5-PLog	0.202482	0.127102	0.099776
6-PLog	0.164542	0.121236	0.099275
AHTan	0.379188	0.193832	0.129178
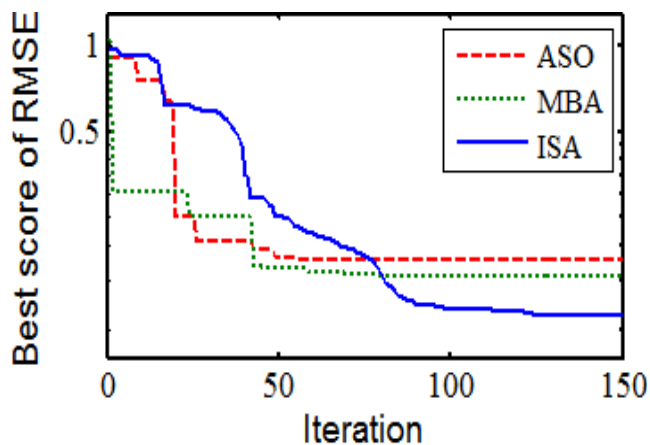
(a) 5-PLog
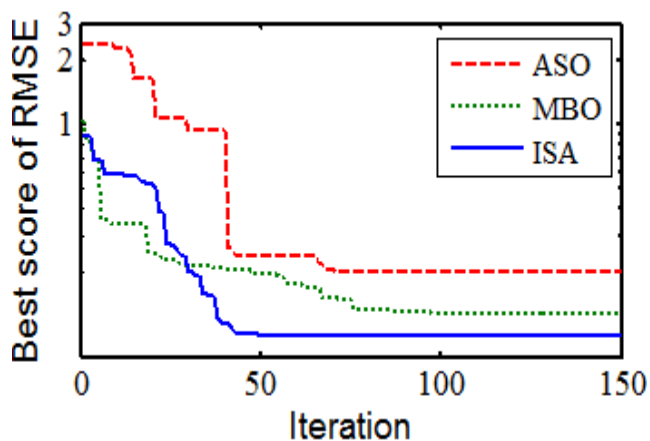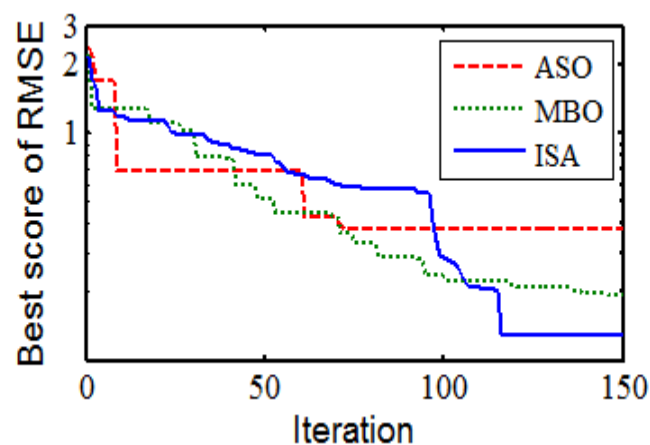

(a) 5-PLog
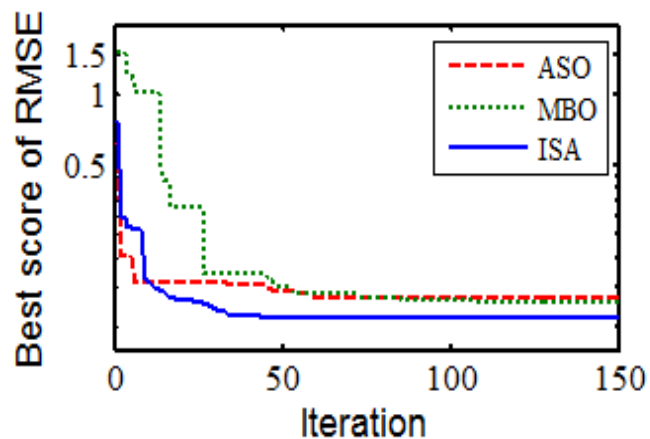
(b) 6-PLog

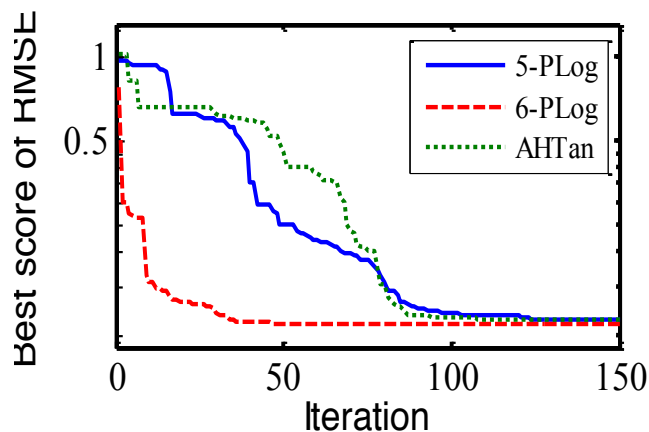

(b) 6-PLog

(c) AHTan

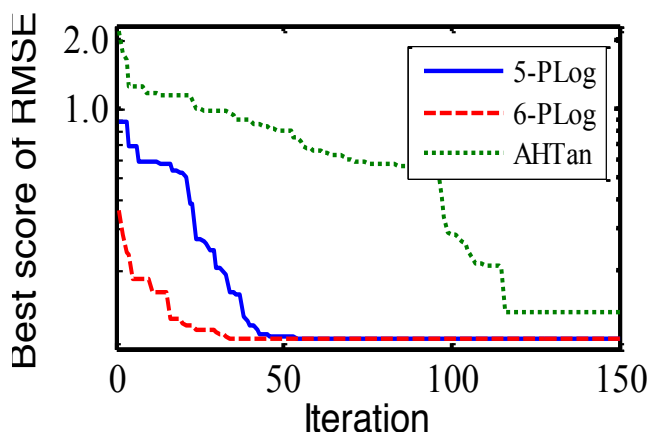(c) AHTan

Figure 3. RMSE convergence of Bazán 62/1300

Figure 4. RMSE convergence of Nordex N117/3600

The estimated P/v plots of WTs using ISA and the realistic data are exposed in Figs. 6 and 7. The existence of estimated P/v curve using ISA in the intermediate of realistic points, corroborates exactness of the identified WTPM parameters.

Execution measures of the ISA are tested by statistical indicators to verify the results forcefulness. The ISA is run 100 independent times and statistical indicators such as Best, Worst, and standard deviation (StD) of RMSE values are recorded in Table 7. It can be affirmed that the smaller values of StD, prove the results forcefulness.

(a) Bazán 62/1300

(b) Nordex N117/3600

Fig. 5 RMSE convergence of 5-PLog, 6-PLog, and AHTan using ISA

Table 7. RMSE statistical results

| WT	Model	RMSE (Best)	RMSE (Worst)	RMSE (StD)
Bazán 62/1300	5-PLog	0.112980	0.119392	0.023967
	6-PLog	0.108789	0.117807	0.031852
	AHTan	0.113243	0.120896	0.026556
Nordex N117/3600	5-PLog	0.099776	0.110237	0.038188
	6-PLog	0.099275	0.104869	0.020673
	AHTan	0.129178	0.138373	0.031222

6. Conclusions

The ISA has two advantages namely ownership of only one parameter and automatic tuning of such parameter. Hence the ISA application to identify WTPM parameters has been innovatively addressed in this article. The purpose of creating an efficient WTPM is to accurately manage and forecast wind energy under different wind speeds. The F_{ob} is to minimize the RMSE among the accompanying computed and measured wind power points of WT with subjection to constraints which are determined by the BB and TB of

parameters. The suggested WTPM effectiveness has been evaluated via comparing its emulated results with the realistic results of two WTs. The emulated results are congruous with the realistic results in all case studies. Moreover, comparisons among the ISA yielded results and other optimizers results have been performed. The ISA-based results reveal that RMSE has decreased by 18.11% to 65.93% from other optimizers and this proves the high competitiveness of ISA to other optimizers. After employing 5-PLog, 6-PLog, and AHTan models, it has been found that the 6-PLog model owns the smallest RMSE and the fastest convergence. Filtering the measured data of WT and utilizing the estimated WTPM for managing and predicting wind energy are proposed issues in future research.
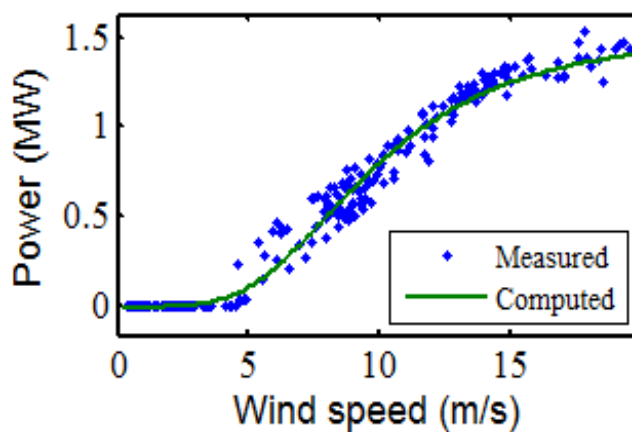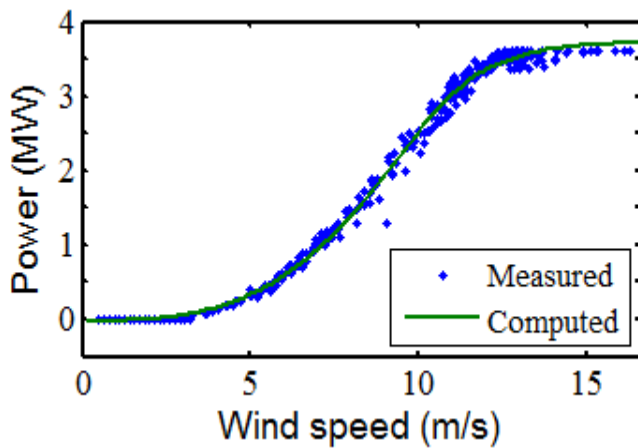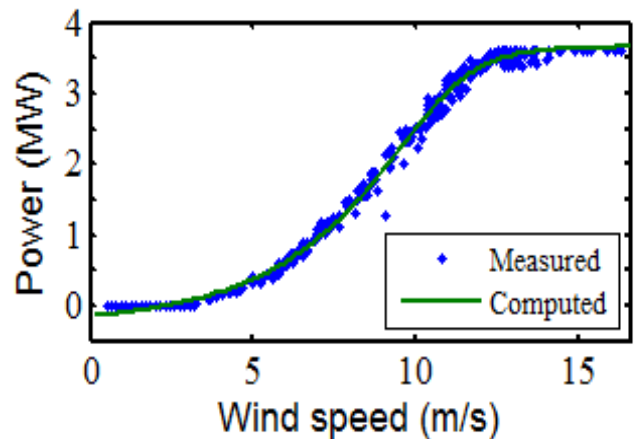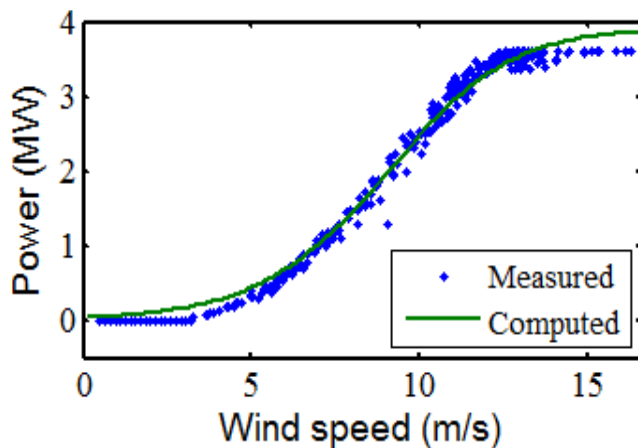

(a) 5-PLog
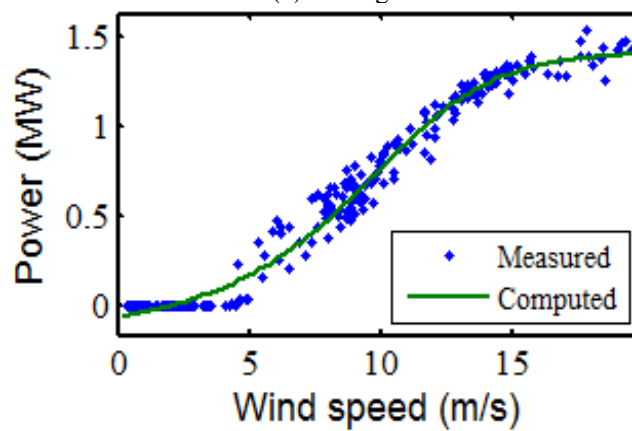
(b) 6-PLog
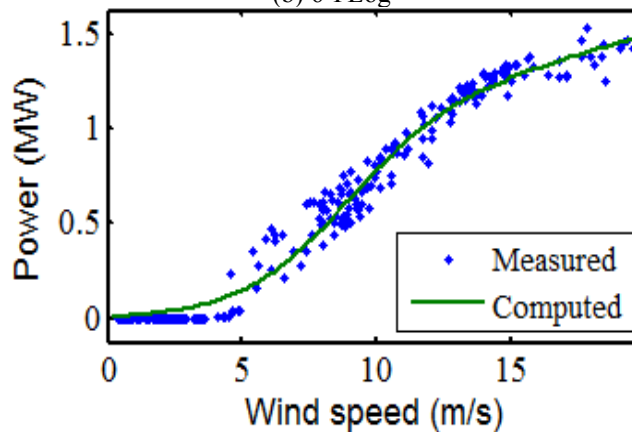
(c) AHTan

Figure 6. P/v plots of Bazán 62/1300

(a) 5-PLog

(b) 6-PLog

(c) AHTan

Figure 7. P/v plots of Nordex N117/3600

References

[1] H. Zhu, M. Sueyoshi, C. Hu, S. Yoshida, "Modelling and attitude control of a shrouded floating offshore wind turbine with hinged structure in extreme conditions", IEEE 6th International Conference on Renewable Energy Research and Applications (ICRERA), San Diego, California, USA, DOI: 10.1109/ICRERA.2017.8191162, pp. 762-767, 5-8 November 2017.

[2] I. R. Mohammed, A. A. Saleh, A. M. Saleh, "Consolidity analysis of wind turbines in wind farms", International Journal of Renewable Energy Research, vol.10, no.1, pp. 205-216, March 2020.

[3] M. Yesilbudak, "Partitional clustering-based outlier detection for power curve optimization of wind turbines", IEEE International Conference on Renewable Energy Research and Applications (ICRERA), Birmingham, UK, DOI: 10.1109/ICRERA.2016.7884500, pp. 1080-1084, 20-23 November 2016.

[4] R. J. A. Vieira, M. A. Sanz-Bobi, "Power curve modelling of a wind turbine for monitoring its behavior", International Conference on Renewable Energy Research and Applications (ICRERA), Palermo, Italy, DOI: 10.1109/ICRERA.2015.7418571, pp. 1052-1057, 22-25 November 2015.

[5] Y. Bao, D. Pan, X. Wang, L. Liao, Q. Yang, "Least-square B-spline approximation based wind turbine power curve modeling", Chinese Automation Congress (CAC), Jinan, China, DOI: 10.1109/CAC.2017.8243986, pp. 6711-6716, 20-22 October 2017.

[6] Y. Bao, Q. Yang, Y. Sun, "Iterative modeling of wind turbine power curve based on least-square B-spline approximation", Asian Journal of Control, DOI: 10.1002/asjc.2150, vol. 21, no. 4, pp. 2004-2016, July 2019.

[7] A. M. Howlader, N. Urasaki, K. Uchida, A. Yona, T. Senjyu, C. Kim, A. Y. Saber, "Parameter Identification of Wind Turbine for Maximum Power-point Tracking Control", Electric Power Components and Systems, DOI: 10.1080/15325000903376974, vol. 38, no. 5, pp. 603-614, March 2010.

[8] A. Goudarzi, I. E. Davidson, A. Ahmadi, G. K. Venayagamoorthy, "Intelligent analysis of wind turbine power curve models", IEEE Symposium on Computational Intelligence Applications in Smart Grid (CIASG), Orlando, Florida, USA, DOI: 10.1109/CIASG.2014.7011548, pp. 1-7, 9-12 December 2014.

[9] A. Kusiak, H. Zheng, Z. Song, "Models for monitoring wind farm power", Renewable Energy, DOI: 10.1016/j.renene.2008.05.032, vol. 34, no. 3, pp. 583-590, March 2009.

[10] M. Lydia, A. I. Selvakumar, S. S. Kumar, G. E. P. Kumar, "Advanced Algorithms for Wind Turbine Power Curve Modeling", IEEE Transactions on Sustainable Energy, DOI: 10.1109/TSTE.2013.2247641, vol. 4, no. 3, pp. 827-835, July 2013.

[11] S. Seo, S. Oh, H. Kwak, "Wind turbine power curve modeling using maximum likelihood estimation method", Renewable Energy, DOI: 10.1016/j.renene.2018.09.087, vol. 136, pp. 1164-1169, June 2019.

[12] A. Goudarzi, A. G Swanson, M. Kazemi, K. Wang, "Intelligent wind turbine power curve modelling using the third version of cultural algorithm (CA3)", International Journal of Renewable Energy Research, vol. 7, no. 3, pp. 1340- 1351, September 2017.

[13] J. Ma, C. Wang, M. Yang, Y. Lin, "Ultra-Short-Term Probabilistic Wind Turbine Power Forecast Based on Empirical Dynamic Modeling", IEEE Transactions on Sustainable Energy, DOI: 10.1109/TSTE.2019.2912270, vol. 11, no. 2, pp. 906-915, April 2020.

[14] J. Zierath, R. Rachholz, S. Rosenow, R. Bockhahn, A. Schulze, C. Woernle, "Experimental identification of modal parameters of an industrial 2-MW wind turbine", Wind Energy, DOI: 10.1002/we.2165, vol. 21, no. 5, pp. 338-356, May 2018.

[15] R. Jin, L. Wang, C. Huang, S. Jiang, "Wind turbine generation performance monitoring with Jaya algorithm", International Journal of Energy Research, DOI: 10.1002/er.4382, vol. 43, no. 4, pp. 1604-1611, March 2019.

[16] M. Marčiukaitis, I. Žutautaitė, L. Martišauskas, B. Jokšas, G. Gecevičius, A. Sfetsos, "Non-linear regression model for wind turbine power curve", Renewable Energy, DOI: 10.1016/j.renene.2017.06.039, vol. 113, pp. 732-741, December 2017.

[17] S. Tao, Q. Xu, A. Feijóo, S. Kuenzel, N. Bokde, "Integrated Wind Farm Power Curve and Power Curve Distribution Function Considering the Wake Effect and Terrain Gradient", Energies, DOI: 10.3390/en12132482, vol. 12, no. 13 2482, June 2019.

[18] M. Yesilbudak, "A novel power curve modeling framework for wind turbines", Advances in Electrical and Computer Engineering, DOI: 10.4316/AECE.2019.03004, vol. 19, no. 3, pp. 29-40, August 2019.

[19] J. Rose, I. A. Hiskens, "Estimating wind turbine parameters and quantifying their effects on dynamic behavior", IEEE Power and Energy Society General Meeting - Conversion and Delivery of Electrical Energy in the 21st Century, Pittsburgh, Pennsylvania, USA, DOI: 10.1109/PES.2008.4596862, pp. 1-7, 20-24 July 2008.

[20] J. Krishna, V. Bhargava, J. Donepudi, "BEM prediction of wind turbine operation and performance", International Journal of Renewable Energy Research, vol. 8, no. 4, pp. 1962-1973, December 2018.

[21] Y. Cao, Q. Hu, H. Shi, Y. Zhang, "Prediction of wind power generation base on neural network in consideration of the fault time", IEEJ Transactions on Electrical and Electronic Engineering, DOI: 10.1002/tee.22853, vol. 14, no. 5, pp. 670-679, May 2019.

[22] T. Demirdelen, P. Tekin, I. O. Aksu, F. Ekinci, "The Prediction Model of Characteristics for Wind Turbines Based on Meteorological Properties Using Neural Network Swarm Intelligence", Sustainability, DOI: 10.3390/su11174803, vol. 11, no. 17, 4803, September 2019.

[23] L. Bai, E. Crisostomi, M. Raugi, M. Tucci, "Wind turbine power curve estimation based on earth mover distance and artificial neural networks", IET Renewable Power Generation, DOI: 10.1049/iet-rpg.2019.0530, vol. 13, no. 15, pp. 2939-2946, November 2019.

[24] M. Bartolomé, F. Sehnke, J. A. Lazzús, I. Salfate, M. Felder, S. Montecinos, "Wind turbine power curve modeling based on Gaussian Processes and Artificial Neural Networks", Renewable Energy, DOI: 10.1016/j.renene.2018.02.081, vol. 125, pp. 1015-1020, September 2018.

[25] G. Ciulla, A. D'Amico, V. D. Dio, V. L. Brano, "Modelling and analysis of real-world wind turbine power curves: Assessing deviations from nominal curve by neural networks", Renewable Energy, DOI: 10.1016/j.renene.2019.03.075, vol. 140, pp. 477-492, September 2019.

[26] E. Taslimi-Renan, M. Modiri-Delshad, M. F. M. Elias, N. A. Rahim, "Development of an enhanced parametric model for wind turbine power curve", Applied Energy, DOI: 10.1016/j.apenergy.2016.05.124, vol. 177, pp. 544-552, September 2016.

[27] F. D. Caro, A. Vaccaro, D. Villacci, "Adaptive Wind Generation Modeling by Fuzzy Clustering of Experimental Data", Electronics, DOI: 10.3390/electronics7040047, vol. 7, no. 4, 47, March 2018.

[28] T. Ouyang, A. Kusiak, Y. He, "Modeling wind-turbine power curve: A data partitioning and mining approach", Renewable Energy, DOI: 10.1016/j.renene.2016.10.032, vol. 102, pp. 1-8, March 2017.

[29] S. Pei, Y. Li, "Wind Turbine Power Curve Modeling with a Hybrid Machine Learning Technique", Applied Sciences, DOI: 10.3390/app9224930, vol. 9, no.22, 4930, November 2019.

[30] R. K. Pandit, D. Infield, "Comparative analysis of Gaussian Process power curve models based on different stationary covariance functions for the purpose of improving model accuracy", Renewable Energy, DOI: 10.1016/j.renene.2019.03.047, vol. 140, pp. 190-202, September 2019.

[31] M. Mehrjoo, M. J. Jozani, M. Pawlak, "Wind turbine power curve modeling for reliable power prediction using monotonic regression", Renewable Energy, DOI: 10.1016/j.renene.2019.08.060, vol. 147, pp. 214-222, March 2020.

[32] A. H. Gandom, "Interior search algorithm (ISA): A novel approach for global optimization", ISA Transactions, DOI: 10.1016/j.isatra.2014.03.018, vol. 53, no. 4, pp. 1168-1183, July 2014.

[33] M. Moravej, S. Hosseini-Moghari, "Large Scale Reservoirs System Operation Optimization: the Interior Search Algorithm (ISA) Approach", Water Resources

Management, DOI: 10.1007/s11269-016-1358-y, vol. 30, no. 10, pp. 3389-3407, August 2016.

[34] M. Kumar,T. K. Rawat, A. Jain, A. A. Singh, A. Mittal, "Design of Digital Differentiators Using Interior Search Algorithm", Procedia Computer Science, DOI: 10.1016/j.procs.2015.07.351, vol. 57, pp. 368-376, August 2015.

[35] B. Bentouati, S. Chettih, L. Chaib, "Interior search algorithm for optimal power flow with non-smooth cost functions", Cogent Engineering, DOI: 10.1080/23311916.2017.1292598, vol. 4, no. 1, 1292598, February 2017.

[36] I. N. Trivedi, P. Jangir, M. Bhoye, N. Jangir, "An economic load dispatch and multiple environmental dispatch problem solution with microgrids using interior search algorithm", Neural Computing and Applications, DOI: 10.1007/s00521-016-2795-5, vol. 30, pp. 2173-2189, October 2018.

[37] K. Khan, A. Kamal, A. Basit, T. Ahmad, H. Ali, A. Ali, "Economic Load Dispatch of a Grid-Tied DC Microgrid Using the Interior Search Algorithm", Energies, DOI: 10.3390/en12040634, vol. 12, no. 4, 634, February 2019.

[38] D. Kler, K. P. S. Rana, V. Kumar, "Parameter extraction of fuel cells using hybrid interior search algorithm", International Journal of Energy Research, DOI: 10.1002/er.4424, vol. 43, no. 7, pp. 2854-2880, June 2019.

[39] E. A. El-Hay, M. A. El-Hameed, A. A. El-Fergany, "Parameters' optimization of SOFC for steady state and transient simulations", Energy, DOI: 10.1016/j.energy.2018.10.038, vol. 166, pp. 451-461, January 2019.

[40] D. Kler, Y. Goswami, K. P. S. Rana, V. Kumar, "A novel approach to parameter estimation of photovoltaic systems using hybridized optimizer", Energy Conversion and Management, DOI: 10.1016/j.enconman.2019.01.102, vol. 187, pp. 486-511, May 2019.

[41] R. J. A. Vieira, M. A. Sanz-Bobi, S. Kato, "Wind turbine condition assessment based on changes observed in its power curve", International Conference on Renewable Energy Research and Applications (ICRERA), Madrid, Spain, DOI: 10.1109/ICRERA.2013.6749721, pp. 31-36, 20-23 October 2013.

[42] B. Hand, A. Cashman, G. Kelly, "An aerodynamic modelling methodology for an offshore floating vertical axis wind turbine", International Conference on Renewable Energy Research and Applications (ICRERA), Palermo, Italy, DOI: 10.1109/ICRERA.2015.7418708, pp. 273-277, 22-25 November 2015.

[43] D. Villanueva, A. E. Feijóo, "Reformulation of parameters of the logistic function applied to power curves of wind turbines", Electric Power Systems Research, DOI: 10.1016/j.epsr.2016.03.045, vol. 137, pp. 51-58, August 2016.

[44] D. Villanueva, A. Feijóo, "Comparison of logistic functions for modeling wind turbine power curves", Electric Power Systems Research, DOI: 10.1016/j.epsr.2017.10.028, vol. 155, pp. 281-288, February 2018.

[45] Y. Wang, Q. Hu, L. Li, A. M. Foley, D. Srinivasan, "Approaches to wind power curve modeling: A review and discussion", Renewable and Sustainable Energy Reviews, DOI: 10.1016/j.rser.2019.109422, vol. 116, 109422, December 2019.

[46] A. H. Gandomi, David A. Roke, "Engineering optimization using interior search algorithm", IEEE Symposium on Swarm Intelligence, Orlando, Florida, USA, DOI: 10.1109/SIS.2014.7011771, pp. 1-7, 9-12 December 2014.